

Giant spontaneous Hall effect and magnetoresistance in $\text{La}_{1-x}\text{Ca}_x\text{CoO}_3$ ($0.1 \leq x \leq 0.5$)

A. V. Samoilov,^{a)} G. Beach, C. C. Fu, and N.-C. Yeh

Department of Physics 114-36, California Institute of Technology, Pasadena, California 91125

R. P. Vasquez

Center for Space Microelectronics Technology, Jet Propulsion Laboratory, California Institute of Technology, Pasadena, California 91109

Results of resistivity and Hall effect measurements in $\text{La}_{1-x}\text{Ca}_x\text{CoO}_3$ ($0.1 \leq x \leq 0.5$) epitaxial films and ceramics are presented. The spontaneous Hall effect in $\text{La}_{1-x}\text{Ca}_x\text{CoO}_3$ (LCCO) is observed for ferromagnetic samples with $x \geq 0.2$. The Hall effect is largest near the magnetic percolation threshold $x=0.2$. For $x=0.2$, the low-field slope of the Hall resistivity, $\rho_{xy}/(\mu_0 H)$, attains a large value of $2 \times 10^{-6} \text{ m}^3/\text{C}$ below the Curie temperature T_c , which may be applied to sensitive low-field detection. Except near the magnetic percolation threshold, the longitudinal resistivity of LCCO decreases with increasing field at all temperatures. Anomalous temperature-dependent magnetoresistance occurs in the sample with $x=0.2$, which may be associated with the spin-state transition in LCCO. © 1998 American Institute of Physics. [S0021-8979(98)26211-6]

I. INTRODUCTION

The perovskite cobaltite oxide $\text{La}_{1-x}\text{Ca}_x\text{CoO}_3$ (LCCO) is ferromagnetic for $x > 0.15$, with the Curie temperature increasing up to $T_c \approx 180 \text{ K}$ for $x=0.3-0.5$ ¹ (see Fig. 1, upper inset). Substitution of divalent Ca for trivalent La in the parent compound LaCoO_3 results in mixed valency of Co ions ($\text{Co}^{3+}/\text{Co}^{4+}$), and chemically doped holes induce ferromagnetism via the double-exchange interaction.²⁻⁴ Both the trivalent and tetravalent cobalt ions are known to exist in multiple spin configurations. For instance, low- and high-spin states for trivalent cobalt ions have the electronic configurations of $t_{2g}^6 e_g^0$ (Co^{III}) and $t_{2g}^4 e_g^2$ (Co^{3+}), with spin $S=0$ and 2, correspondingly.^{5,6} In LaCoO_3 , the crystal-field splitting energy is larger than the Hund's energy, and the trivalent Co ions are in the low-spin state at low temperatures. Divalent Ca ions in $\text{La}_{1-x}\text{Ca}_x\text{CoO}_3$ polarize the oxygen p electrons and stabilize the high-spin configuration of trivalent Co ions because of the reduced crystal-field effect. As a result, magnetic clusters are formed near each divalent atom. With the increasing doping concentration, the clusters reach magnetic and conducting percolation threshold. A similar system, $\text{La}_{1-x}\text{Sr}_x\text{CoO}_3$, is found to have metallic electrical conduction for $0.3 \leq x \leq 0.5$, with "hole-poor", lower-spin matrix interpenetrating the metallic "hole-rich", higher-spin regions.^{5,6} In this work, we report the observations of a giant ferromagnetic Hall effect and magnetoresistance in LCCO. The possible physical origin of these phenomena is discussed in the context of magnetic clusters and spin transitions due to the multiple spin configurations of the cobaltites.

II. EXPERIMENT

The transport properties are studied in LCCO epitaxial films ($x=0.2, 0.3$, and 0.5) and in a LCCO $x=0.1$ ceramic

sample. The films, $(2-5) \text{ mm} \times (2-5) \text{ mm} \times (100-300) \text{ nm}$ in size, are grown by pulsed laser deposition using stoichiometric targets of LCCO, in 100 mTorr of oxygen. The temperature of the LaAlO_3 substrates is $700 \text{ }^\circ\text{C}$. The growth is followed by annealing in 1 atm oxygen at $900 \text{ }^\circ\text{C}$ for 10 h, and the epitaxy of the films is confirmed by x-ray rocking curves. The results for the $x=0.5$ samples⁷ are very similar to those for the $x=0.3$ sample and are not shown here. The ceramic sample, $6.1 \text{ mm} \times 2.8 \text{ mm} \times 1.7 \text{ mm}$ in size, is cut from the LCCO target with $x=0.1$. The magnetic field is applied perpendicular to the plane of the largest dimensions. Details of transport measurements are given in Ref. 7.

III. RESULTS

Figure 1 shows the temperature (T) dependence of the electrical resistivity ρ in zero magnetic field. The sample

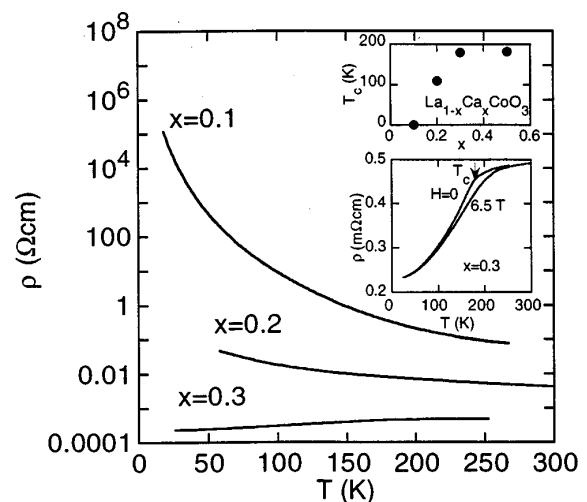


FIG. 1. (Upper panel) The resistivity vs temperature for the $x=0.1$ ceramic sample and for the two epitaxial films (with $x=0.2$ and 0.3). Upper inset: the doping dependence of the transition temperature $T_c(x)$ in $\text{La}_{1-x}\text{Ca}_x\text{CoO}_3$. Lower inset: $\rho(T)$ dependence for $\text{La}_{0.7}\text{Ca}_{0.3}\text{CoO}_3$ in magnetic fields 0 and 6.5 T.

^{a)}Electronic mail: samoliov@cco.caltech.edu

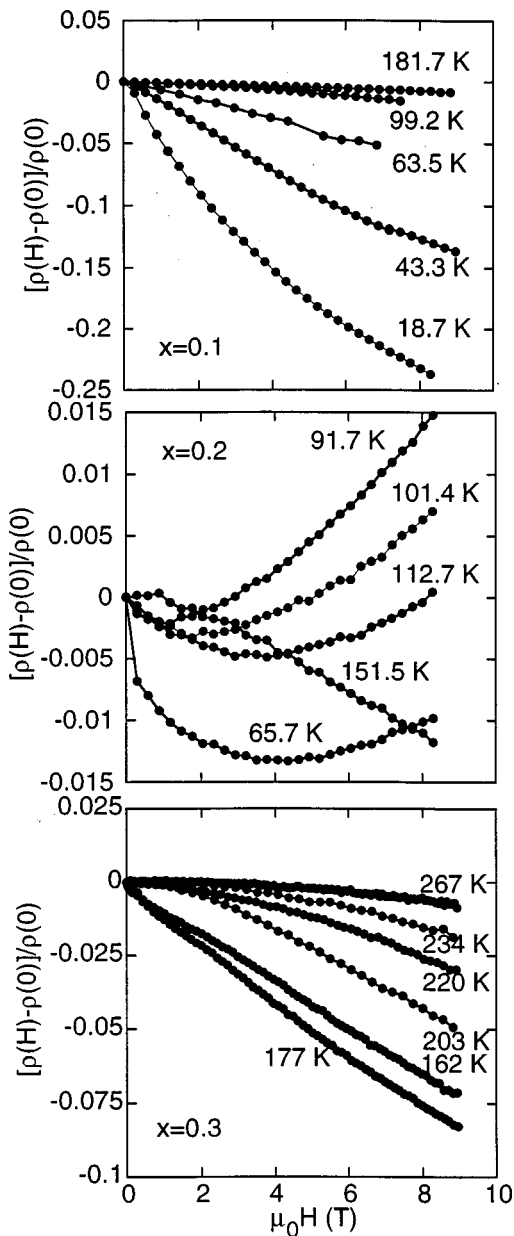


FIG. 2. (Upper panel) The magnetic field dependences of the longitudinal resistivity for $x=0.1$, 0.2 , and 0.3 . The temperature is indicated near each curve. Solid lines are guides to the eye.

with $x=0.3$ exhibits metalliclike resistivity. Below T_c , increasing magnetic order with decreasing temperature decreases carrier scattering and therefore results in a large decrease in the resistivity on cooling through T_c (Fig. 1, lower inset). The resistivity of the samples with $x=0.2$ and 0.1 has semiconductinglike behavior (Fig. 1, main panel), which has been attributed to trapping of holes at the divalent doping ions.⁵

The magnetic field (H) dependence of the resistivity is depicted in Fig. 2. The origin of the negative magnetoresistance for $x=0.3$ can be understood in terms of conventional behavior for metallic ferromagnets, where the magnetoresistivity is due to the suppression of the spin-disorder scattering, which is strongest near the transition temperature, see Fig. 2, bottom panel.

For the ceramic $x=0.1$ sample (Fig. 2, top panel), the magnetoresistance is also negative, and at low temperatures attains relatively larger values (up to 25%) than those of the metallic samples. Unlike samples with high concentration of the Ca atoms, which demonstrate bulk ferromagnetism, the $x=0.1$ sample consists of isolated clusters containing Co^{3+} and tetravalent cobalt ions. These clusters are localized at the Ca ions at low temperatures. The electrical conduction occurs via the hopping motion of holes in the insulating matrix of low-spin, trivalent Co^{III} ions. Each hopping process consists of transferring the tetravalent configuration $[\text{Co}^{\text{IV}} (S=1/2)]$ or $\text{Co}^{4+} (S=5/2)]$ from one Co ion to another, accompanied by transforming of the neighboring Co^{III} ions into Co^{3+} ions.⁵ With increasing temperature, the ratio of Co^{3+} to Co^{III} ions in the matrix increases, facilitating the hopping process and increasing the conductivity. On the other hand, the presence of an external magnetic field helps aligning the spins of Co^{3+} and $\text{Co}^{4+}(\text{Co}^{\text{IV}})$ ions, thereby increasing the hopping rate and resulting in negative magnetoresistivity. With increasing temperature, the correlations between the spins of Co^{3+} and $\text{Co}^{4+}(\text{Co}^{\text{IV}})$ ions become weaker, therefore larger fields are required to align the spins, and the magnetoresistance decreases (Fig. 2, top panel). We note that the magnetoresistance data on LCCO with $x=0.1$ and 0.3 are consistent with those on $\text{La}_{1-x}\text{Sr}_x\text{CoO}_3$ with the same doping levels.⁸

On the other hand, the LCCO sample with $x=0.2$ exhibits an anomalous magnetoresistance behavior (Fig. 2, middle panel), which has not been seen in $\text{La}_{1-x}\text{Sr}_x\text{CoO}_3$. The relative change of the resistivity with the magnetic field $[\rho(H) - \rho(0)]/\rho(0)$ in LCCO with $x=0.2$ is of the order of 1%, smaller than that for $x=0.3$ (Fig. 2, bottom panel). At high temperatures ($T > \approx 120$ K), the magnetoresistance is negative over the whole field range. At lower temperatures, the resistivity as a function of the increasing magnetic field exhibits a nonmonotonic behavior (Fig. 2, middle panel): the initial decrease at small fields is followed by an increase at larger fields. This positive upturn contribution to the resistivity at high fields increases as the temperature is lowered (compare the isotherms at $T=112.7$, 101.4 , and 91.7 K in Fig. 2, middle panel). However, when the temperature decreases further, the negative contribution grows substantially, and the positive upturn in the ρ -vs- H curves becomes less pronounced. (See the isotherm at $T=65.7$ K in Fig. 2, middle panel.) The complexity of the magnetoresistivity behavior in LCCO with $x=0.2$ may be related to the closeness of T_c to the temperature where the $\text{Co}^{3+}/\text{Co}^{\text{III}}$ ratio in the intercluster matrix reaches 50:50 (≈ 110 K, according to Ref. 5). This novel behavior in the magnetoresistance of LCCO awaits further theoretical investigations. We also note that the occurrence of the nonmonotonic field dependence of the resistivity coincides with the temperature interval in which the giant spontaneous Hall effect is observed. (See Ref. 7, Fig. 3, and the discussion below.)

Figure 3 is a representative result of the Hall effect measurements on LCCO with $x=0.2$. In our previous work,⁷ we have demonstrated that the Hall resistivity in LCCO for $0.2 \leq x \leq 0.5$ is proportional to the magnetization M : $\rho_{xy}(H, T) = R_s(T)[\mu_0 M(H, T)]$, where R_s is the spontaneous Hall co-

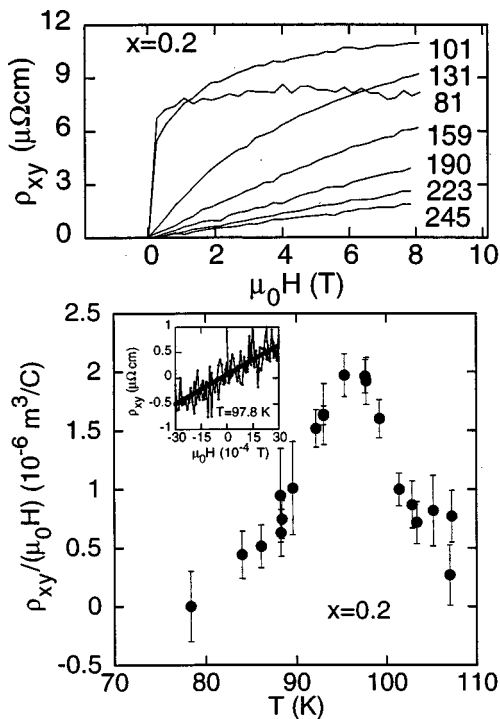


FIG. 3. Top panel: The Hall resistivity vs magnetic field for a $x=0.2$ epitaxial film sample. The temperature is indicated near each curve in Kelvins. Note a very steep rise of ρ_{xy} at low fields and at $T < T_c \approx 110$ K. Bottom panel: The initial slope of the ρ_{xy} -vs- H curves as a function of temperature below $T_c \approx 110$ K for a $x=0.2$ epitaxial film sample. Inset: ρ_{xy} -vs- H at low fields for the same sample at $T=97.8$ K.

efficient, and μ_0 is the permeability of vacuum. The spontaneous Hall coefficient in LCCO peaks nearest the transition temperature, with $R_s(T_c) \approx 0.25 \times 10^{-6} \text{ m}^3/\text{C}$ for $x=0.3$ and 0.5 and $1.35 \times 10^{-6} \text{ m}^3/\text{C}$ for $x=0.2$. The latter value is the largest for known ferromagnetic metals.⁷ For $x=0.1$, no Hall effect signal can be detected within our instrumental resolution. As illustrated in Fig. 3, the ρ_{xy} -vs- H curves for $x=0.2$ becomes progressively more nonlinear as the temperature is decreased in the paramagnetic state above $T_c \approx 110$ K. In the ferromagnetic state, the Hall resistivity as a function of H is found to be hysteretic.⁷ If the sample is cooled in $H=0$, the Hall resistivity at $T < T_c$ shows a very sharp rise with increasing magnetic field, consistent with alignment of magnetic domains. We investigate this initial increase of $\rho_{xy}(H)$ by using a small copper coil to supply small fields up to $\pm 30 \times 10^{-4}$ T (Fig. 3, bottom panel, inset). Within this magnetic field range, the Hall resistivity is linear with field and is reversible. The temperature dependence of the slope $\rho_{xy}/(\mu_0 H)$ is shown in the main panel of Fig. 3. (We note that $\rho_{xy}/(\mu_0 H)$ should not be confused with R_s : $\rho_{xy}/(\mu_0 H) = R_s M/H = R_s \chi$, where χ is the susceptibility.) The slope increases with the increasing temperature,

passes through a maximum $\rho_{xy}/(\mu_0 H) \approx 2 \times 10^{-6} \text{ m}^3/\text{C}$ at $T \approx 97$ K and drops to $5 \times 10^{-8} \text{ m}^3/\text{C}$ at $T = 110$ K. (The latter value is inferred from measurements over a larger field range.) The peaking behavior of $\rho_{xy}/(\mu_0 H)$ -vs- T in the ferromagnetic state is due to the decreasing susceptibility and increasing spontaneous Hall coefficient R_s with the increasing temperature.

In order to appreciate the large magnitude of the slope $\rho_{xy}/(\mu_0 H)$ in LCCO with $x=0.2$, we estimate the “effective” carrier density n , had the Hall effect in LCCO been entirely due to the Lorentz force rather than the magnetization. Using $\rho_{xy}/(\mu_0 H) = 1/(ne)$, where e is the electron charge, we obtain a small value $n = 3 \times 10^{24} \text{ m}^{-3}$, comparable to that in sensitive semiconducting Hall-effect magnetometers.

The spontaneous Hall effect in magnetic materials is generally associated with the spin-orbit interaction.^{9,10} In LCCO, the spin-orbit interaction in the ferromagnetic state may be further enhanced at the boundaries between the low-spin, low-conduction and the high-spin, high-conduction regions.

In summary, the $\text{La}_{1-x}\text{Ca}_x\text{CoO}_3$ system exhibits novel behavior in the magnetoresistance for $x=0.2$ and a very large spontaneous Hall effect at $x \geq 0.2$. These phenomena may be attributed to a magnetism associated with the coexistence of multiple spin configurations in the cobaltites. On the practical side, our finding of the giant Hall effect in these cobaltites appears promising for applications to sensitive low-field magnetometers.

ACKNOWLEDGMENTS

The research at Caltech is jointly supported by the National Aeronautics and Space Administration, Office of Space Science (NASA/OSS), Caltech President’s Fund, and the Packard Foundation. Part of the research was performed at the Center for Space Microelectronics Technology, Jet Propulsion Laboratory, Caltech, and was sponsored by NASA/OSS. A.V.S. is a Millikan Senior Research Fellow in Physics.

¹H. Taguchi, M. Shimada, and M. Koizumi, *J. Solid State Chem.* **41**, 329 (1982).

²G. H. Jonker and J. van Santen, *Physica (Amsterdam)* **16**, 337 (1950).

³C. Zener, *Phys. Rev.* **82**, 403 (1960).

⁴P.-G. de Gennes, *Phys. Rev.* **118**, 141 (1960).

⁵M. A. S  nris-Rodr  guez and J. B. Goodenough, *J. Solid State Chem.* **118**, 323 (1995).

⁶M. Itoh *et al.*, *J. Phys. Soc. Jpn.* **63**, 1486 (1994).

⁷A. V. Samoilov, N.-C. Yeh, and R. P. Vasquez, *Mater. Res. Soc. Symp. Proc.* **474**, 247 (1997); A. V. Samoilov *et al.* (to be published).

⁸R. Mahendiran and A. K. Raychaudhuri, *Phys. Rev. B* **54**, 16 044 (1996).

⁹C. M. Hurd, *The Hall Effect in Metals and Alloys* (Plenum, New York, 1972).

¹⁰A. Fert and D. K. Lottis, in *Concise Encyclopedia of Magnetic and Superconducting Materials* (Oxford University, New York, 1992), p. 287.